Research Project - Characterization Of a Control System For Scramjet Engine Combustor

Shavit Attar and Dan Michaels
Faculty of Aerospace Engineering, Technion - Israel Institute of Technology

This project provides a comprehensive review of control strategies for the Dual-Mode Scramjet (DMSJ) engine, a propulsion system that transitions between ramjet and scramjet modes to operate efficiently across supersonic and hypersonic speeds. Fundamental DMSJ dynamics and mechanisms are explored, including mode transition, wall pressure profiles, shock train location, flame stabilization modes, distributed fuel injection schemes, and their interdependencies. Additionally, methods for shock train location detection using pressure transducers are reviewed, as well as control methods like proportional-derivative (PD) control and all-coefficient-adaptive-control (ACAC). Closed-loop control systems were shown to control shock train location in ramjet mode successfully. Still, shock train location control under scramjet conditions and controlled mode transition were yet to be demonstrated.

I. Introduction

There has been a growing interest in hypersonic flight in recent years, defined by flight at a Mach number exceeding 5. Contrary to turbojet and turbofan engines, designed to produce thrust at the subsonic and low-supersonic regions (blow Mach number of 2), ramjet and scramjet (supersonic combustion ramjet) engines are air-breathing engines designed to operate and the most efficient propulsion method in term of specific impulse above Mach number of 2. While traditionally, rockets have been used to achieve hypersonic Mach numbers, they are less efficient than air-breathing engines because they must carry onboard oxidizers and cannot utilize the surrounding air for combustion. This is evident in figure 1 [1] when comparing specific impulses, which indicates system efficiency. As shown in figure 1 [1], the ramjet engine is the most efficient in the high-supersonic range, whereas the scramjet engine is the most efficient in the hypersonic range.

Both engines belong to the family of open Brayton cycles. The ramjet engine achieves air compression by a change of the inner geometry of the inlet and diffuser. A series of oblique shockwaves leading to a final normal shockwave compress incoming air and decelerate the flow to subsonic velocities. This process exchanges kinetic energy for enthalpy and the pressure rises. Subsequently, combustion takes place in the subsonic flow after which the flow is accelerated through a nozzle generating thrust [2]. At hypersonic Mach numbers, decelerating the flow to subsonic velocities decreases efficiency significantly. This is a result of the very high stagnation enthalpy of the air, limiting the

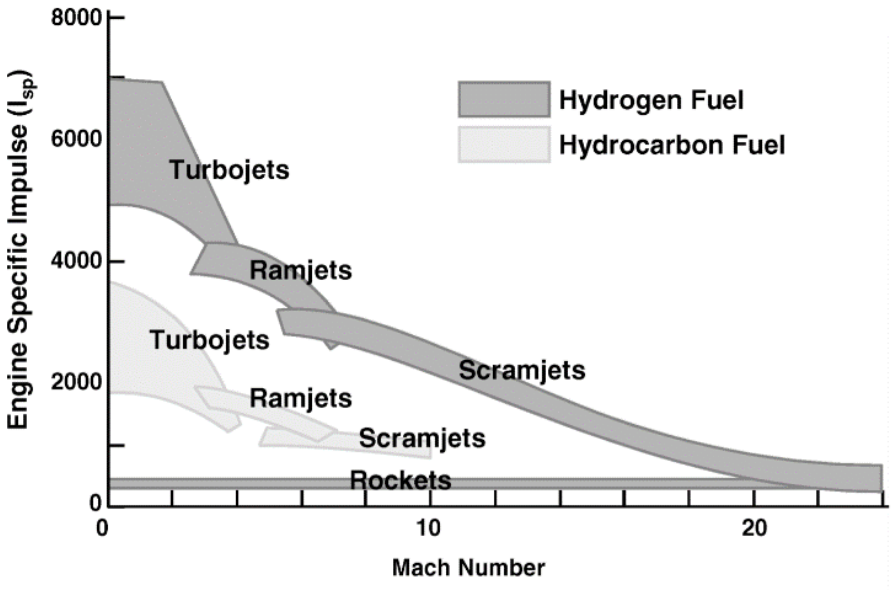

Fig. 1 The specific impulse for different engine concepts and fuel types [1]

enthalpy increase from the combustion process and the large stagnation pressure loss caused by the high Mach number shockwaves [3]. By keeping the flow supersonic, we decrease the stagnation pressure losses and keep the air enthalpy before combustion lower, thus allowing a more significant enthalpy increase through the combustion process.

In the scramjet engine, as illustrated in figure 2 [4], an oblique shock at the front of the vehicle provides initial compression, further compression is achieved through a series of oblique shockwaves in the inlet. During combustion, local pressure rises and the boundary layer separates from the combustion chamber walls, leading to the formation of a series of oblique shockwaves in the isolator section, often referred to as a "shock train". Through the shock train, the pressure and temperature increase and the flow decelerates to a lower Mach number before entering the combustor. The main purpose of the isolator section is to contain the effects of combustion and prevent the shock train from traveling upstream and out of the inlet [5]. As a result of the supersonic flow at the inlet of the combustor, the combustion in the

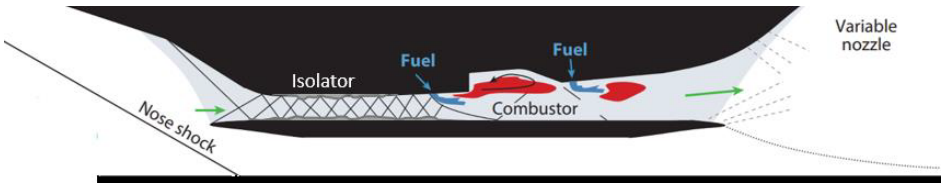

Fig. 2 Schematic of a cavity-based scramjet combustor [4].

scramjet engine must take place in supersonic conditions, leading to an effective residence time of about a millisecond in the combustor. For this reason, the combustor is equipped with a flame holder, creating a region where the conditions allow for a sustained reaction. Due to its great efficiency over a wide range of operating conditions, a cavity flame holder is commonly used in supersonic combustors [6, 7]. The cavity generates a region of subsonic, turbulent flow,

which increases residence time and traps hot combustion products, helping to sustain the reaction.

II. Dynamics in Dual Mode Scramjets

The Dual-Mode Scramjet (DMSJ) is a special type of scramjet that can operate in both subsonic and supersonic combustion conditions using the same engine geometry [8]. This allows the DMSJ to benefit from the high efficiency of a ramjet when accelerating at supersonic Mach numbers and then transition to supersonic combustion to operate efficiently at hypersonic Mach numbers [9].

DMSJ can operate like a traditional scramjet, compressing the air with an oblique shock train, adding heat through combustion in the combustor, usually using a cavity flame holder, and accelerating the air again through an expanding nozzle. Similar to a Rayleigh flow, if the combustion process adds sufficient heat, the flow will thermally choke, meaning it reaches Mach 1 due to heat addition. When the flow is thermally choked, a normal shock train is formed in the isolator section, resulting in a subsonic core flow in the combustor [10]. A thermally choked operation is referred to as "Ramjet mode" while an unchoked operation is referred to as "Scramjet mode".

Three main flame stabilization modes can be observed in a DMSJ with a cavity flame holder, shown in Figure 3 [11]: "Cavity-Assisted Jet Wake-Stabilized Flame", "Cavity Shear Layer-Stabilized Flame" and "Combined Shear Layer, Jet Wake-Stabilized Flame". Micka and Driscoll [12] studied the combustion process in a DMSJ model with a 50/50 blend of hydrogen and ethylene injected upstream of the cavity flame holder and direct fueling from the cavity rear wall. When the combustor operated at thermally choked conditions (ramjet mode) the "Cavity-Assisted Jet Wake-Stabilized Flame" was typically observed, When operated at scramjet mode, the flame stabilized within the cavity shear layer - "Cavity Shear Layer-Stabilized Flame". They also observed an intermediate state where the flame oscillated between the fuel jet-wake and the cavity shear layer. In experiments where the upstream fuel injector was moved closer to the cavity leading edge, the flame was pushed further downstream resulting in a "Combined Shear Layer, Jet Wake-Stabilized Flame".

Fotia and Driscoll [13] examined ram-scram transition using a direct-connect DMSJ model experiment along with pressure measurements and high-speed laser interferometry. Figure 4 shows the pressure measurements for decreasing equivalence ratios, corresponding to decreasing fuel flow. In cases A1 to A4, pressure increases in the isolator, but decreases in the combustor in the downstream direction, indicating that the combustion is subsonic. Subsonic combustion drives the Mach number upward toward unity while driving the static pressure downward in the downstream direction. Ram-scram transition occurs when the pressure profile abruptly decreases between Case A4 (ram) and A5 (scram). As seen in Figure 4, Case A5 displays almost no pressure rise in the isolator because the flow isn't thermally choked, thus a normal shock train doesn't form. Note that for Case A5 the pressure rises in the combustor, a characteristic of supersonic combustion.

Figure 5 [13] shows the dependence of the combustion mode (Ram/Scram) on the equivalence ratio and the

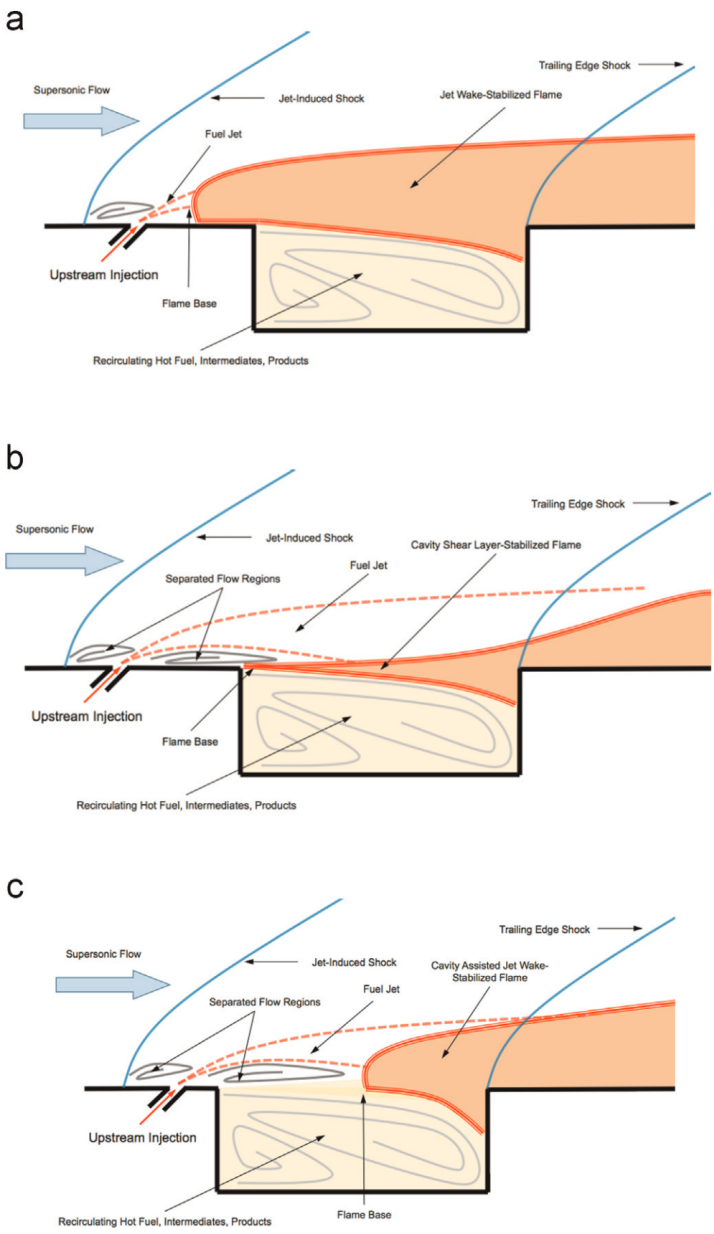

Fig. 3 Common flame stabilization modes in a cavity-based dual-mode scramjet [11]

Case	Mode	T_o	ϕ	r
	kPa	K		
A1	Ram	1400	0.337	1.421
A2	Ram	1400	0.286	1.285
A3	Ram	1400	0.257	1.210
A4	Ram	1400	0.224	1.109
A5	Scram	1400	0.187	0.990
A6	—	1400	0	0

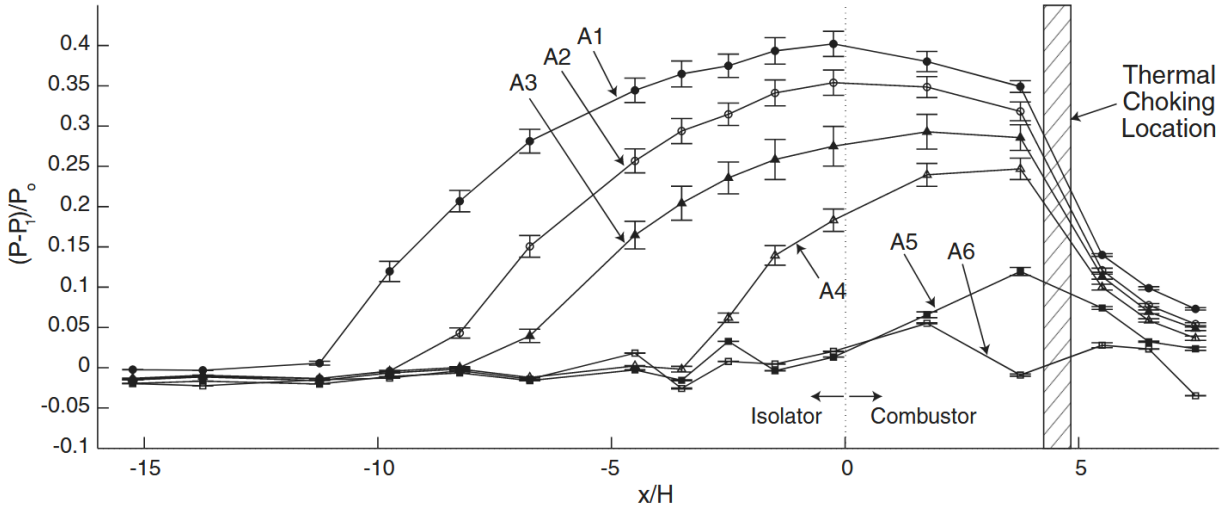

Fig. 4 Experiment conditions and static pressure traces of ram-scram transition by decreasing equivalence ratio ϕ for steady conditions [13].

connection between the engine mode and the flame stabilization mode. These results indicate that the DMSJ mode and the shock train are strongly linked with the magnitude, position, and distribution of released heat.

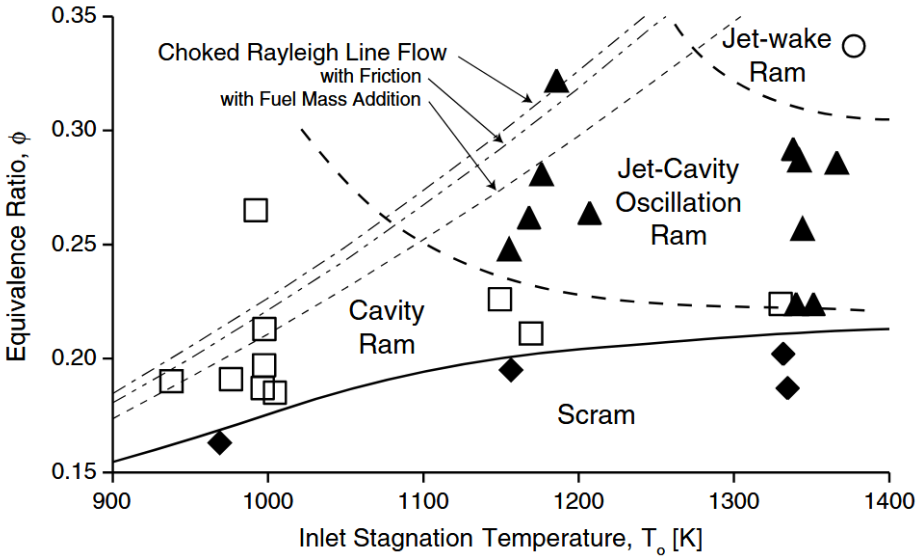

Fig. 5 Flame stabilization modes as a function of inlet stagnation temperature T_0 and fuel-equivalence ratio ϕ [13].

Yokev et al. [14] investigated the impact of fuel injection distribution on flame stabilization and heat release in a cavity-stabilized DMSJ. Ethylene was injected using two fuel injection locations, one upstream of the cavity and another in the cavity. Several different fuel injection distributions were tested. It was found that when the cavity fuel flow rate was low, the flame stabilized on the cavity shear layer and resulted in a gradual pressure rise in the combustor. A sufficiently high fuel flow rate in the cavity led to flame stabilization upstream of the cavity, in the fuel jet wake, and a more confined combustion zone. It was concluded that the heat release distribution and pressure profile in the combustor could be significantly influenced by the fuel injection distribution through its impact on the flame stabilization mode.

Kanapathipillai et al. [15] looked at a different approach to fuel injection distribution using a direct-connect,

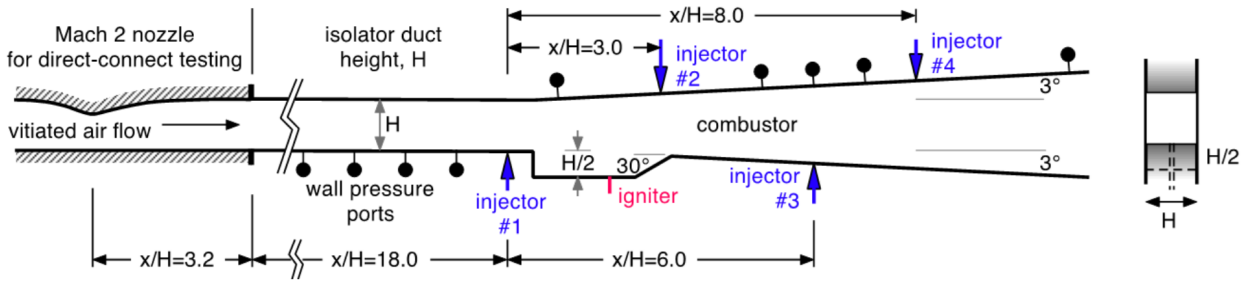

Fig. 6 Dual-mode scramjet schematic [15].

cavity-stabilized DMSJ model. Gaseous hydrogen was injected through one to four injectors using a distributed fuel injection scheme (Figure 6 [15]) while keeping a constant global equivalence ratio. As shown in Figure 7 [15], the

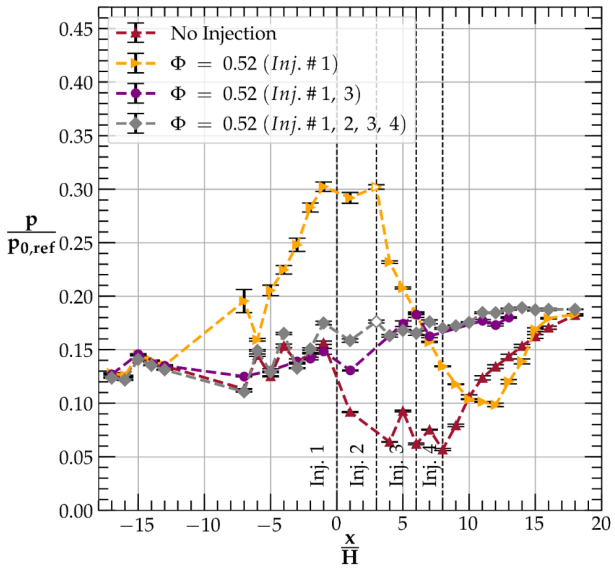

Fig. 7 Pressure distributions comparing single injection to distributed injection [15].

distributed fuel injection schemes are characterized by a gradual pressure rise across the combustor as opposed to the abrupt, strong pressure rise observed in the cavity region of the thermally-choked single injection case. This indicates that in the cases of distributed fuel injection despite injecting a similar amount of fuel as the thermally-choked case, the combustor is operating in supersonic combustion mode.

III. Control

Controlling the shock train location in a DMSJ is important for several reasons. Firstly, as shown in the previous section, there is a strong link between the shock train location and the mode of operation of a DMSJ. Secondly, positioning the shock train near the cavity was shown to enhance fuel mixing and, consequently, improve combustion efficiency [16]. Finally, control over the shock train location could aid in preventing "Unstart", a phenomenon that occurs when the shock train moves upstream of the isolator section and into the inlet, resulting in poor engine performance and damage to the airframe or vehicle instability [17].

Closed-loop control over the shock train location requires a method for measuring the shock train location and a method for varying its location.

A. Shock train detection

Several approaches have been investigated for the real-time detection of the shock train location.

Le et al. [18] used time-resolved pressure measurements in a dual-mode scramjet isolator to investigate the potential for using the measurements for shock train leading-edge detection. Three detection criteria were defined and examined: 1) 150% of the normalized pressure magnitude at the isolator inlet, 2) 150% of the normalized pressure standard deviation

level at the isolator inlet, and 3) the maximum value of the normalized pressure standard deviation. Another method of shock train leading-edge detection involved the examination of the frequency content of the pressure signal using power spectra analysis. Results indicated that the second detection criterion provided the earliest method of shock train detection as the shock train moved upstream, followed by the first and third criteria.

Donbar et al. [19] examined methods of shock-train leading-edge detection using an array of high-frequency pressure transducers located in the isolator/combustor region of a direct-connect hydrocarbon-fueled, scramjet combustor. Similarly to Le et al. [18], a threshold, standard deviation, and spectral approach were examined. Furthermore, Donbar et al. [19] implemented a "sum of pressures" approach that summed the total isolator pressure to give a shock train location, which they found more reliable and faster than the other methods. The advantage of the sum of pressures approach is that it is integrative, which reduces noise and is more robust in the event of sensor failure.

Vanstone et al. [20] took a different approach. They developed a simple physics-based model based on the fact that the shock train was shown to manifest at the location within the isolator that possesses the Mach number required to match the isolator pressure ratio - the ratio of isolator exit pressure to inlet pressure. Using the normal-shock and quasi-one-dimensional isentropic-flow equations, a relation was derived for determining the location of the leading shock of the shock train. The model performed well using only the Mach-number-gradient information in a Mach 1.8 cold-flow direct-connect isolator, but not as well in a combusting Mach 2.2 direct-connect dual-mode scramjet tunnel. Improved performance of the model for both tunnels was achieved with the use of more calibration data.

B. closed-loop control

Only a few attempts at closed-loop control of the shock train location in a combusting DMSJ have been made. Vanstone et al. [21] demonstrated the closed-loop control of a shock train location in the isolator of a Mach 2.2 direct-connect dual-mode scramjet operating on liquid fuel in ramjet mode. The control task was to move the shock train to a user-selected location. Several algorithms for shock train location were tested including a threshold method that relied on wall-pressure measurements in the isolator. The isentropic flow equations are used to estimate the pressure jump across a normal shock in a Mach 2.2 flow, and the shock location is estimated as the location where the wall pressure exceeds 60% of the estimated pressure jump. A flap is used to modulate the backpressure, and hence affect the shock train location in the isolator, as shown in Figure 8 [21]. A proportional-derivative (PD) control design was used to move the shock train to a selected location (Figure 9 [21]). As can be seen in Figure 10 [21], the PD controller performed well when the shock location was measured by an array of pressure transducers.

A more advanced control approach was explored by Rockwell et al. [22]. The use of an adaptive control approach known as characteristic model-based all-coefficient adaptive control (ACAC) was explored using a simple, semi-empirical model of a dual-mode scramjet. Prior knowledge of the scramjet plant is not required for the all-coefficient adaptive control, and it is predicted that this controller can better perform when changes in the plant take place. When

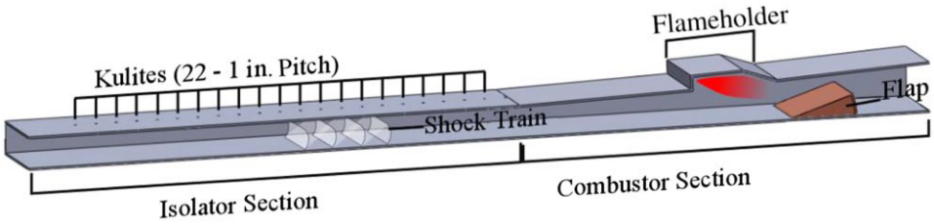

Fig. 8 Simplified schematic of the direct-connect dual-mode scramjet [21].

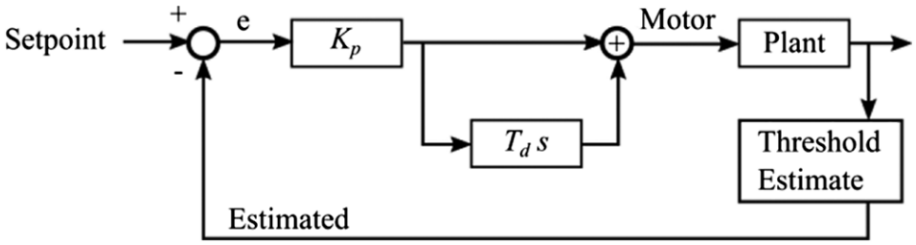

Fig. 9 PD control using threshold shock estimate [21].

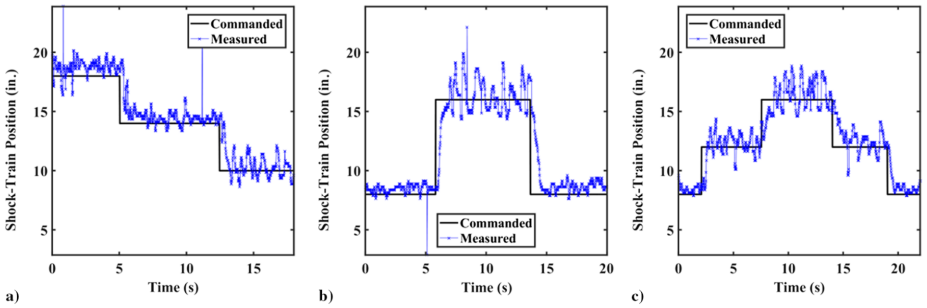

Fig. 10 Shock train location control using PD [21].

characteristics of the plant deviate from their nominal values, the adaptive controller can adjust in real-time and maintain a stable system response. Figure 11 [22] shows the results of the shock train control simulation with a change in the valve static gain. This type of change could be due to a drop in inlet mass capture or pressure, a change in flowpath geometry or inlet distortion, or a combination of these factors that result in a longer shock train without a corresponding increase in the fuel flow delivered by the valve. As can be seen in Figure 11 [22], unlike the PID, the ACAC is more stable and displays no oscillation in its response. It was concluded that the ACAC is better able to accommodate changes in the plant.

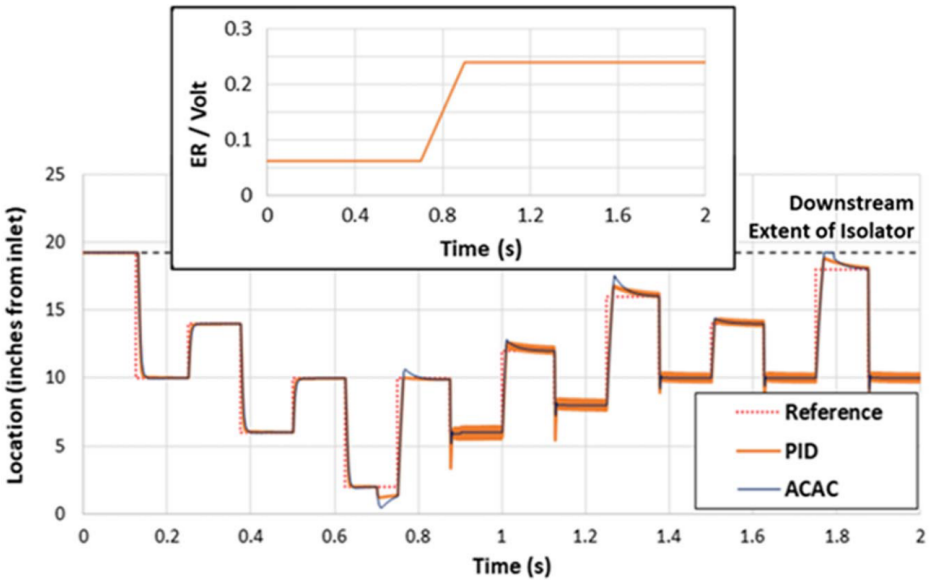

Fig. 11 Shock train tracking with a linear change in the valve static gain [22].

IV. Conclusion

This project presents an overview of the ramjet, scramjet, and dual-mode scramjet engines, and their respective advantages, challenges, and limitations. The basic working principles of a DMSJ are explained, such as ram and scram modes, shock train, thermal choking, and cavity flame holder. This project also provides a review of studies exploring DMSJ dynamics and mechanisms, including mode transition, wall pressure profiles, shock train location, flame stabilization modes, different fuel injection schemes, and the connection between all of those factors.

The motivation for a closed-loop control system for the DMSJ is presented and several measurement and control approaches are reviewed.

While closed-loop control of the shock train location in ramjet mode was successfully demonstrated in past research, control over the shock train location in scramjet mode and controlled mode transition were yet to be shown. Furthermore, the continuous change in fuel injection distribution as a dynamic control variable for a closed-loop control system hasn't been studied yet.

References

[1] Fry, R. S., "A Century of Ramjet Propulsion Technology Evolution," *Journal of Propulsion and Power*, Vol. 20, No. 1, 2004, pp. 27–58. https://doi.org/10.2514/1.9178, URL https://doi.org/10.2514/1.9178, publisher: American Institute of Aeronautics and Astronautics _eprint: https://doi.org/10.2514/1.9178.

[2] THOMAS, A. N., "Some Fundamental Aspects of Ramjet Propulsion," *Journal of Jet Propulsion*, Vol. 27, No. 4, 1957, pp. 381–385. https://doi.org/10.2514/8.12787, URL https://doi.org/10.2514/8.12787, publisher: American Institute of Aeronautics and Astronautics _eprint: https://doi.org/10.2514/8.12787.

[3] Segal, C., *The Scramjet Engine: Processes and Characteristics*, Cambridge University Press, 2009. Google-Books-ID: kPMhAwAAQBAJ.

[4] Urzay, J., "Supersonic Combustion in Air-Breathing Propulsion Systems for Hypersonic Flight," *Annual Review of Fluid Mechanics*, Vol. 50, No. Volume 50, 2018, 2018, pp. 593–627. https://doi.org/10.1146/annurev-fluid-122316-045217, URL https://www-annualreviews-org.ezlibrary.technion.ac.il/content/journals/10.1146/annurev-fluid-122316-045217, publisher: Annual Reviews.

[5] Smart, M. K., "Scramjet isolators," *AVT-185 AVT/VKI Lecture Series, von Kármán Inst. RTO-EN-AVT-185-AC/323 (AVT-185) TP/375, Rhode St. Genèse, Belgium*, 2010. URL https://www.sto.nato.int/publications/STO%20Educational%20Notes/RTO-EN-AVT-185/EN-AVT-185-10.pdf.

[6] Ben-Yakar, A., and Hanson, R. K., "Cavity Flame-Holders for Ignition and Flame Stabilization in Scramjets: An Overview," *Journal of Propulsion and Power*, Vol. 17, No. 4, 2001, pp. 869–877. https://doi.org/10.2514/2.5818, URL https://doi.org/10.2514/2.5818, publisher: American Institute of Aeronautics and Astronautics _eprint: https://doi.org/10.2514/2.5818.

[7] Mathur, T., Gruber, M., Jackson, K., Donbar, J., Donaldson, W., Jackson, T., and Billig, F., "Supersonic Combustion Experiments with a Cavity-Based Fuel Injector," *Journal of Propulsion and Power*, Vol. 17, No. 6, 2001, pp. 1305–1312. https://doi.org/10.2514/2.5879, URL https://doi.org/10.2514/2.5879, publisher: American Institute of Aeronautics and Astronautics _eprint: https://doi.org/10.2514/2.5879.

[8] Heiser, W. H., and Pratt, D. T., *Hypersonic Airbreathing Propulsion*, AIAA, 1994. Google-Books-ID: d1sQvT2_kMsC.

[9] Billig, F. S., "Research on supersonic combustion," *Journal of Propulsion and Power*, Vol. 9, No. 4, 1993, pp. 499–514. https://doi.org/10.2514/3.23652, URL https://doi.org/10.2514/3.23652, publisher: American Institute of Aeronautics and Astronautics _eprint: https://doi.org/10.2514/3.23652.

[10] Curran, E. T., Heiser, W. H., and Pratt, D. T., "Fluid phenomena in scramjet combustion systems," *Annual Review of Fluid Mechanics*, , No. 28, 1996, pp. 323–360. URL https://dialnet.unirioja.es/servlet/articulo?codigo=5550791, publisher: Annual reviews.

[11] Barnes, F. W., and Segal, C., "Cavity-based flameholding for chemically-reacting supersonic flows," *Progress in Aerospace Sciences*, Vol. 76, 2015, pp. 24–41. https://doi.org/10.1016/j.paerosci.2015.04.002, URL https://www.sciencedirect.com/science/article/pii/S0376042115000317.

[12] Micka, D., and Driscoll, J., "Reaction Zone Imaging in a Dual-Mode Scramjet Combustor Using CH-PLIF," *44th AIAA/ASME/SAE/ASEE Joint Propulsion Conference & Exhibit*, American Institute of Aeronautics and Astronautics, Hartford, CT, 2008. https://doi.org/10.2514/6.2008-5071, URL http://arc.aiaa.org/doi/abs/10.2514/6.2008-5071.

[13] Fotia, M. L., and Driscoll, J. F., "Ram-Scram Transition and Flame/Shock-Train Interactions in a Model Scramjet Experiment," *Journal of Propulsion and Power*, Vol. 29, No. 1, 2013, pp. 261–273. https://doi.org/10.2514/1.B34486, URL https://doi.org/10.2514/1.B34486, publisher: American Institute of Aeronautics and Astronautics _eprint: https://doi.org/10.2514/1.B34486.

[14] Yokev, N., Brod, H. E., Cao, D., and Michaels, D., "Impact of Fuel Injection Distribution on Flame Holding in a Cavity-Stabilized Scramjet," *Journal of Propulsion and Power*, Vol. 37, No. 4, 2021, pp. 584–594. https://doi.org/10.2514/1.B38093, URL https://doi.org/10.2514/1.B38093, publisher: American Institute of Aeronautics and Astronautics _eprint: https://doi.org/10.2514/1.B38093.

[15] Kanapathipillai, M., "Scramjet Combustor Mode Transition by Controlling Fuel Injection Distribution," PhD Thesis, University of Maryland, College Park, 2022. URL https://search.proquest.com/openview/86c4a3e16b9fc54a277e9be2ebe6e90d/1?pq-origsite=gscholar&cbl=18750&diss=y.

[16] Menon, S., "Shock-wave-induced mixing enhancement in scramjet combustors," 1989. URL https://ntrs.nasa.gov/citations/19890037720, nTRS Author Affiliations: Flow Research, Inc. NTRS Report/Patent Number: AIAA PAPER 89-0104 NTRS Document ID: 19890037720 NTRS Research Center: Legacy CDMS (CDMS).

[17] Curran, E. T., "Scramjet Engines: The First Forty Years," *Journal of Propulsion and Power*, Vol. 17, No. 6, 2001, pp. 1138–1148. https://doi.org/10.2514/2.5875, URL https://doi.org/10.2514/2.5875, publisher: American Institute of Aeronautics and Astronautics _eprint: https://doi.org/10.2514/2.5875.

[18] Le, D. B., Goyne, C. P., and Krauss, R. H., "Shock Train Leading-Edge Detection in a Dual-Mode Scramjet," *Journal of Propulsion and Power*, Vol. 24, No. 5, 2008, pp. 1035–1041. https://doi.org/10.2514/1.32592, URL https://doi.org/10.2514/1.32592, publisher: American Institute of Aeronautics and Astronautics _eprint: https://doi.org/10.2514/1.32592.

[19] Donbar, J., Linn, G., and Akella, M., "High-Frequency Pressure Measurements for Unstart Detection in Scramjet Isolators," *46th AIAA/ASME/SAE/ASEE Joint Propulsion Conference & Exhibit*, American Institute of Aeronautics and Astronautics, 2010. https://doi.org/10.2514/6.2010-6557, URL https://arc.aiaa.org/doi/abs/10.2514/6.2010-6557, _eprint: https://arc.aiaa.org/doi/pdf/10.2514/6.2010-6557.

[20] Vanstone, L., Lingren, J., and Clemens, N. T., "Simple Physics-Based Model for the Prediction of Shock-Train Location," *Journal of Propulsion and Power*, Vol. 34, No. 6, 2018, pp. 1428–1441. https://doi.org/10.2514/1.B37031, URL https://doi.org/10.2514/1.B37031, publisher: American Institute of Aeronautics and Astronautics _eprint: https://doi.org/10.2514/1.B37031.

[21] Vanstone, L., Hashemi, K. E., Lingren, J., Akella, M. R., Clemens, N. T., Donbar, J., and Gogineni, S., "Closed-Loop Control of Shock-Train Location in a Combusting Scramjet," *Journal of Propulsion and Power*, Vol. 34, No. 3, 2018, pp. 660–667. https://doi.org/10.2514/1.B36743, URL https://doi.org/10.2514/1.B36743, publisher: American Institute of Aeronautics and Astronautics _eprint: https://doi.org/10.2514/1.B36743.

[22] Rockwell, R., Goyne, C., Di, L., Lin, Z., Bakos, R., and Donbar, J., "Simulated Scramjet Shock Train Control Using an All-Coefficient Adaptive Control Approach," *Journal of Propulsion and Power*, Vol. 39, No. 4, 2023, pp. 492–500. https://doi.org/10.2514/1.B38827, URL https://doi.org/10.2514/1.B38827, publisher: American Institute of Aeronautics and Astronautics _eprint: https://doi.org/10.2514/1.B38827.